

Distribution and Susceptibility Assessment of Collapses and Landslides in the Riparian Zone of the Xiaowan Reservoir

ZHONG Ronghua^{1,2}, HE Daming^{1,2}, HU Jinming^{1,2}, DUAN Xingwu^{1,2}, HUANG Jiangcheng^{1,2}, CHENG Xupeng^{1,2}

(1. Institute of International Rivers and Eco-security, Yunnan University, Kunming, 650091, China; 2. Yunnan Key Laboratory of International Rivers and Transboundary Eco-security, Yunnan University, Kunming, 650091, China)

Abstract: The southwest alpine gorge region is the major state base of hydropower energy development in China and hence planned many cascading hydropower stations. After the reservoir impoundment, the intense water level fluctuations under the interaction of cascade dams operating and the mountainous flooding, usually cause bank collapse, landslide and debris flow hazards. The Xiaowan reservoir (XWR), for example, as the ‘dragon head’ meg reservoir located in the middle mainstream of Lancang River, have resulted in a series of geohazards during its building and operating. In this study, we investigated the number and surface area of collapses and landslides (CLs) occurred in the water level fluctuations zone (WLFZ) of XWR using remote sensing images of Gaofen-1 and Google Earth; evaluated the CLs susceptibility using information value method. The results presented that the total WLFZ area of 87.03 km² and 804 CLs masses with a total area of 1.98 km² were identified in the riparian zone of XWR. CLs mainly occurred at an elevation of 1190–1240 m, and the CLs density increased with an increase in altitude. The WLFZ with a slope gradient of 25°–45° is the main CLs distribution area that accounts for more than half of the total CLs area. The susceptibility assessment revealed that high and very high susceptibility zones are generally distributed along zones with an elevation of 1210–1240 m, a slope degree of 25°–45° and a slope aspect perpendicular to the direction of Lancang River. Furthermore, these susceptible zones are close in distance to the dam site and tend to be in the riparian zones with the formation lithology of Silurian strata. These results provide a valuable contribution to prevent and control geohazards in the XWR area. Moreover, this study offers a constructive sample of geohazards assessment in the riparian zone of large reservoirs throughout the mountains of southwest China.

Keywords: susceptibility assessment; collapses and landslides; water level fluctuations; Xiaowan Reservoir; Lancang-Mekong River

Citation: ZHONG Ronghua, HE Daming, HU Jinming, DUAN Xingwu, HUANG Jiangcheng, CHENG Xupeng, 2019. Distribution and Susceptibility Assessment of Collapses and Landslides in the Riparian Zone of the Xiaowan Reservoir. *Chinese Geographical Science*, 29(1): 70–85. https://doi.org/10.1007/s11769-018-1012-0

1 Introduction

As more and more large dams have been constructed on mountainous rivers to satisfy the world’s growing energy demand, bank erosion has become a major concern subsequent to the reservoir impoundment (Cyberski, 1973; Chai, 1996; Fu et al., 2010; Butt et al., 2011; Xu

et al., 2013; Bao et al., 2015; Tang et al., 2016; Zhong et al., 2016; Su et al., 2017). Bank erosion, including landslide and bank collapse, occurs within the littoral zone of reservoir directly damage the hydraulic structures (Wang et al., 2007; Alimohammadlou et al., 2013). Specifically, large rock-soil masses fall into the reservoir at high-speed cause surges and thus seriously threaten the

Received date: 2018-01-31; accepted date: 2018-04-28

Foundation item: Under the auspices of the National Natural Science Foundation of China (No. 41601296) and National Key R&D Program of China (No. 2016YFA0601601), China Postdoctoral Science Foundation (No. 2016M592720), Yunnan Applied Basic Research Projects (No. 2016FD11)

Corresponding authors: HE Daming. E-mail: dmhe@ynu.edu.cn; HU Jinming. E-mail: hujm@ynu.edu.cn

© Science Press, Northeast Institute of Geography and Agroecology, CAS and Springer-Verlag GmbH Germany, part of Springer Nature 2018

safe operation of the dam, as well as the lives and property of people around the reservoir (Song et al., 2015; Jiang et al., 2016). Furthermore, the rock-soil masses discharged into the reservoir leads to sedimentation and consequential decrease in the dam's effective storage capacity (Jiang et al., 2016). One of the most catastrophic bank failures on record was the disastrous landslide of the Vaiont Reservoir on the Piave River, Italy, in 1963, which caused deadly consequences with more than 2000 fatalities (Barla and Paronuzzi, 2013). Subsequent to the Vaiont landslide disaster, the impact of reservoir impoundment on bank stability has been widely investigated and acknowledged (Fujita, 1977; Saint-Laurent et al., 2001; Zhang et al., 2006; Wang and Yan, 2007; Luo et al., 2008; Paronuzzi et al., 2013; Johansson and Edeskär, 2014; Yang et al., 2014; Xia et al., 2015; Kaczmarek et al., 2016; Sun et al., 2017a; 2017b). It is evident that the construction of water conservancy projects and reservoir impoundment are critical factors that cause collapses and landslides (CLs), therefore the geohazards in any reservoir area pose an important threat to the productive life and the safe operation of the reservoir (Paronuzzi and Bolla, 2012; Xia et al., 2013; Yuan et al., 2013; Song et al., 2015; Babanouri and Dehghani, 2017; Zhou et al., 2017). In general, bank erosion is mainly caused by natural factors, such as heavy rainfall and earthquakes, anthropogenic activities, such as deforestation, road operation, mining and construction (Iverson, 2000; Pradhan and Lee, 2010; Xu et al., 2012; Alimohammadlou et al., 2013; Duan et al., 2016). However, the failure of the bank in a reservoir is mainly caused by the periodic alternation of drying and wetting of the riparian zone, according to water level regulations (Xia et al., 2013; Johansson and Edeskär, 2014; Wang et al., 2014; Yang et al., 2014; Jiang et al., 2016; Sun et al., 2017b). With the impoundment of the reservoir, the potential sliding surface at the bottom of the rock slope is softened or muddied along with the rising groundwater level, increase pore water pressure and subsequently decrease the bank's sheer strength (Fujita, 1977; Yan et al., 2010; Xia et al., 2015). Meanwhile, the changed pore pressure and surface water pressure because of the water level fluctuations (WLFs) together with the decreasing shear strength of the rock-soil body further affect the bank stability (Liao et al., 2005; Luo et al., 2008; Jia et al., 2009). These factors contribute to a decrease in slope stability after res-

ervoir impoundment, particularly when there is rapid drawdown in the water level, which ultimately results in bank failures (Xia et al., 2015). In addition, after the reservoir operation, existing vegetation in the riparian zone starts to decay and the root systems decompose, eliminating the soil consolidation. These factors coupled with the wave scouring bank toe induced by wind and shipping, the riparian zone has thus been noted to easily generate geological disasters in particular regarding bank collapses and landslides (Liao et al., 2005; Wang and Yan, 2007; Zhou et al., 2010; Bao et al., 2011, 2015; Wu et al., 2013).

In China, to meet the growing demand of energy consumption, and to alleviate air pollution and mitigate the effects of global climate change, the pace of hydropower development accelerated in recent years (Chang et al., 2010; Tang et al., 2013; 2017). Meanwhile, with the increasing number of large hydropower stations, the geohazards along the reservoir area have become a wide concern and many investigations have been conducted into bank failures related to WLFs during the operation of a reservoir. Among these projects, the Three Gorges Project has attracted the most consideration. The impoundment of the Three Gorges Reservoir (TGR) caused many geological hazards around the reservoir area, especially landslides and bank collapses, leading to numerous assessment reports about hazards susceptibility and bank stability analyses (Wu et al., 2001; 2004; Zhou et al., 2010; Huang et al., 2012; Xia et al., 2013; Wang et al., 2014; Chen et al., 2015a; 2016). Nonetheless, most investigations were limited to a single landslide or specific bank segment, studies regarding the entire reservoir have not been considered. Actually, most of the collapses and all the fronts of landslides occurred in the zone of reservoir inundation, where is most intensively disturbed by water level regulation. This area is also known as the water-level-fluctuating zone (WLFZ), which refers to the area along the reservoir bank that is limited by the maximum and minimum water levels (Tang et al., 2014; Bao et al., 2015). Thus, the WLFZ is defined as a unique geomorphic unit which is formed by long-term alternating periods of being either flooded or dry, according to the reservoir's water level regulation (Bao et al., 2015). There is currently still a lack of research on geohazards in the WLFZ, although some researchers have reported the geohazards along the WLFZ of the TGR.

The Xiaowan Reservoir (XWR) is the first ‘dragon head’ reservoir of the cascade hydropower dams in mainstream of Lancang River (LCR). Since the full impoundment in 2012, an artificial riparian zone with a vertical height of 60 m has been created in XWR. The comprehensive actions of periodical submersion and exposure, as well as the local mountainous flooding have caused severe soil erosion and ecological degradation triggering the unstable steep bank to become prone to collapses and landslides. Such eco-environmental changes and subsequent rise in the potential for geological disasters threaten the safety of lives and property around the reservoir area as well as the safe operation of the Xiaowan Dam (XWD). These problems have garnered high attention from the reservoir management department and local government. Thus, scientific research into the eco-environmental degradation in the riparian zone of the XWR is required. Owing to the complicated terrain and sparse population, attention and research related to the XWR is particularly limited. Recently, some scholars have explored the bank collapse pattern and mechanism (Li, 2011; Wu, 2011), bank stability (Liu et al., 2011; Li, 2012), and the landslide and its potential harm along the XWR (Wang, 2012). However, these investigations have focused on a single hazard point or specific hazard incident without regard for the reservoir in its entirety and the potential for geological disaster in the WLFZ.

This study evaluated the spatial distribution of WLFZ and susceptibility of CLs along the entire riparian zone in the XWR using the information value method. This work aims to provide some reference for geological disaster prevention and control along the riparian zone of the XWR. Moreover, this study will help to provide profound insights into the research and management of the other large reservoirs in the southwest alpine gorge region of China.

2 Methods

2.1 Study area

The Xiaowan dam is located in 1.5 km downstream of the junction between the mainstream of LCR and Heihui River (HHR), downstream of the Gongguoqiao dam and upstream of the Manwan dam (Fig. 1). The Xiaowan project construction started in October 2004 and filling began in December 2008, it become the second largest

power station in the planned cascading hydropower dams of the Lancang River Basin (LCRB), with an installed capacity of 4200 MW and characterized by respective crest length of 892.8 m and dam height of 294.5 m. The longest backwater length of the LCR and HHR is 179.6 km and 125.3 km, respectively. The total storage capacity of XWR is about $150 \times 10^9 \text{ m}^3$ with a normal water level of 1240 m; its regulated storage capacity is $99 \times 10^8 \text{ m}^3$, depending on seasonal discharge regulations (Chen et al., 2015c). The XWR covers an area of 189.1 km² over eight districts and is mainly distributed in Fengqing, Changning, Longyang and Nanjian counties. The elevation of mountains surrounding the reservoir is above 2200 m. The regional climate is semi-tropical monsoon, with an annual precipitation of 770 mm to 1330 mm and annual average temperature ranging between 14.3°C to 19°C (Wu et al., 2014).

2.2 Dataset

In this study, a digital elevation model (DEM) with 10 m spatial resolution of the XWR provided by Huaneng Lancang River Hydropower Co., Ltd, was used to extract the WLFZ distribution. The Gaofen-1 Landsat image, with 8 m spatial resolution for panchromatic and 16 m spatial resolution for multi-spectral imaging (April 2014) covering the total XWR area, was used to distinguish CLs points. In addition, a DEM with 30 m spatial resolution of Yunnan Province was created to ascertain the watershed boundary and stream networks of the XWR. DEM and Landsat images were projected using the UTM WGS 84 zones, 47°N. We also used Google Earth images (dated April 2014) to discern the positions of CLs.

2.3 Identification of water-level-fluctuating zone and collapses and landslides of the Xiaowan Reservoir

2.3.1 WLFZ and CLs identification

The XWR has comprehensive benefits such as flooding control, sediment trapping and navigation, although it is mainly utilized for power generation. According to the annual operation program of the XWR, a typical hydrological year consists of five stages: 1) the water level drops gradually from 1240 m to 1180–1186 m during January to March due to drought and in order to drain the reservoir; 2) the water level is maintained at an approximately constant minimum level of 1180 m from

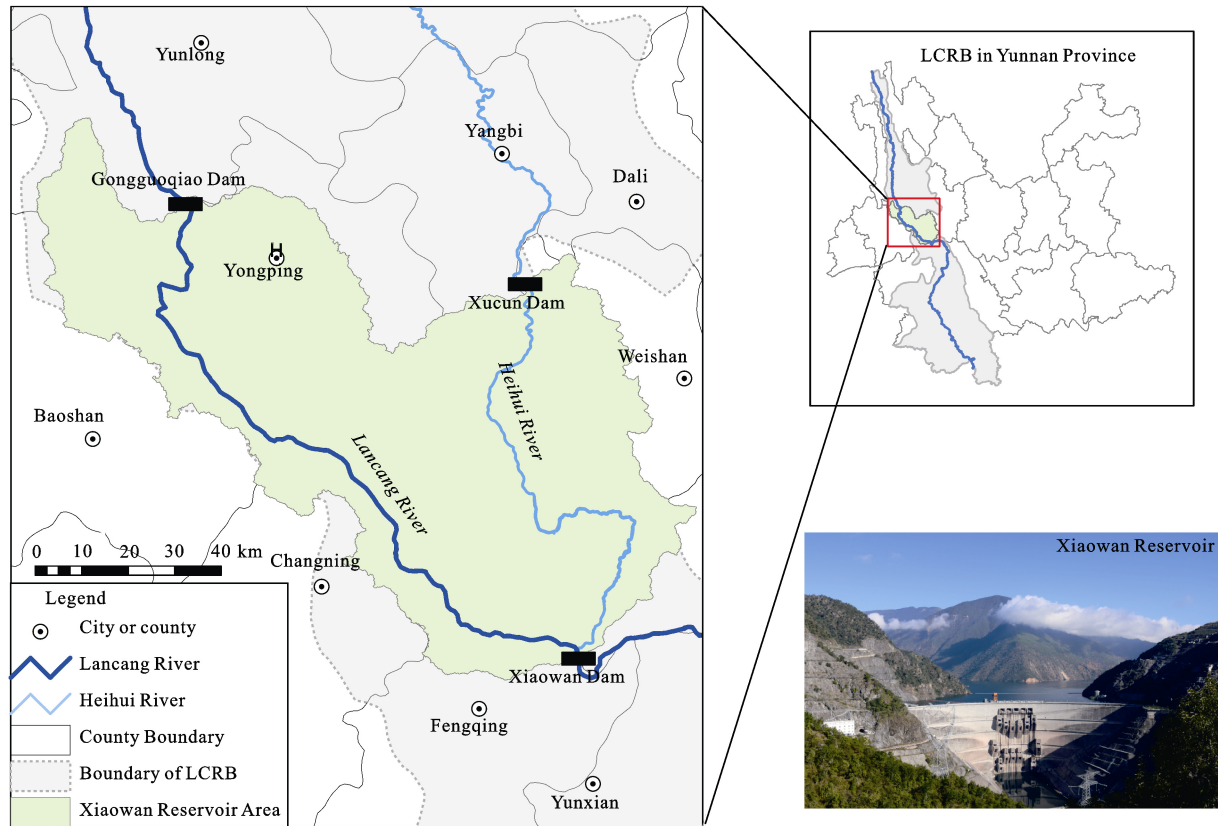


Fig. 1 Location of the Xiaowan dam and the Xiaowan Reservoir in the Lancang River (LCRB, Lanchang River Basin)

April to May to discharge the muddy water; 3) the reservoir is operated to control the water level at lower than 1232 m for flood control during June to mid-September, and raised to between 1232 m to 1240 m during mid-September to late October; and 5) the reservoir is fully impounded with a constant maximum level of approximately 1240 m during November to December (Fig. 2). Consequently, over the years, an artificial riparian zone with a vertical height of 60 m has been cre-

ated. Owing to the changes in the river's longitudinal elevation, the vertical height of the WLFZ gradually decreases from the dam site to the terminal of the back-water, which is the natural river channel. In present study, we used the DEM of the XWR with 10 m resolution to extract the WLFZ. The highest and the lowest water level elevations remained 1240 m and 1180 m respectively. Furthermore, the projection areas of the WLFZ in different ranges were calculated.

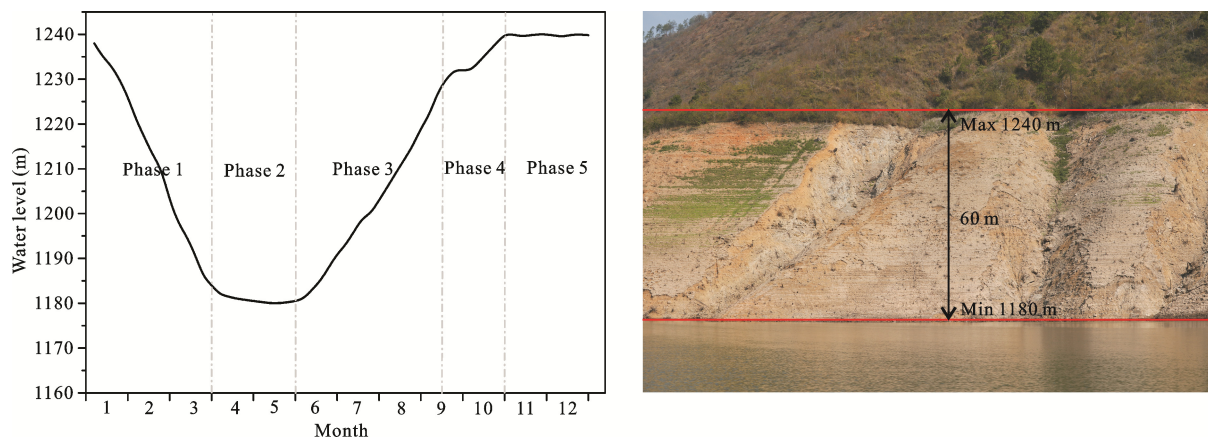
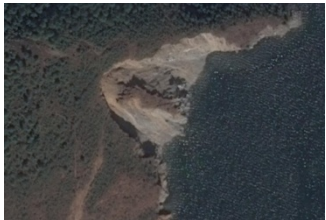
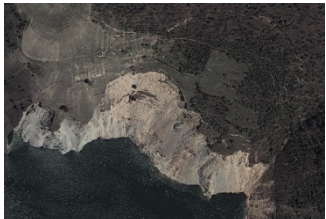
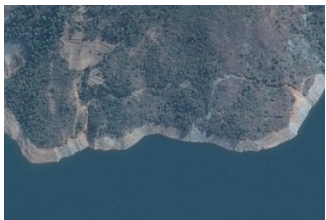



Fig. 2 Water level regulation and the water-level-fluctuating zone in the Xiaowan Reservoir

Meanwhile, the GF-1 and Google Earth images along the XWR were used to investigate the CLs occurring in the riparian zone. The CLs masses were identified using the image features exhibited in Table 1 and checked with the actual CLs data from the field inves-

tigation of bank erosion from May to June in 2015 and 2016. It is important to note that the CLs investigated in the present study include the masses whose backscarps were located upland of the WLFZ but whose fronts were in the riparian zone (Fig. 3).

Table 1 The image characteristics of bank failure and landslide

Interpreting marks	Image features	Example
Structure of rock and soil	A loose perturbation of rock-soil block is often seen on the bank; the rock-soil layer and the attitude of rock are not continuous with the surrounding rock-soil.	
Geomorphic features	The shape of the slope is often a horseshoe or round-backed armchair; the front platform of bank is wide owing to having been flattened and there is a subsidence phenomenon with a high trailing edge on a steep wall. There are often multistage staggered platforms with developed surface fractures, and deep cuts of natural dissected valleys on both sides, sometimes dissecting the valleys' consanguinity.	
Boundary features	In the trailing edge of the steep wall, there is a mark along the direct slope; the two sides are bound by cracks or gullies; the front edges display ligule protuberances, usually a small collapse or rock pile.	
Vegetation cover	The slope is bare or with sparse vegetation, significantly different from the surrounding vegetation.	

2.3.2 Calculations of WLFZ and CLs spatial distribution

CLs density, which refers to the ratio of the area of CLs to the area of the WLFZ, was calculated at different spatial classes and factors. Generally, CLs is influenced by many environmental and man-made factors, such as lithology, elevations, slope gradients, slope aspects, and climate (Dai and Lee 2002; Lee and Sambath, 2006; Park 2010; Yilmaz 2010; Yalcin et al. 2011; Xu et al. 2012; Guo et al. 2015). In this investigation, the area of WLFZ and CLs distributed in different elevations, slope gradients, slope aspects, and distances to dam site

were analyzed based on the DEM and Remote images. The elevation was divided into six classes with 10 m intervals from 1180 m to 1240 m. The slope gradient was divided into five classes, specifically, gentle slope (0° – 15°), moderately steep slope (15° – 30°), steep slope (25° – 35°), high steep slope (35° – 45°) and cliff ($>45^{\circ}$). The slope direction also has important influence on the occurrence of CLs. The slope direction was classified as Flat (F), North (N), NE (Northeast), E (East), SE (Southeast), S (South), SW (Southwest), W (West) and NW (Northwest). Distance to dam site is another important factor as along the river, longitudinally from the



Fig. 3 Examples of landslides (a, b, c, d; Yellow dotted line represents the trailing edge of landslide) and collapses (e, f, g, h, i, j) in the riparian zone of the Xiaowan Reservoir

tail to the head of the reservoir, the range of WLFs change according to the reduction of channel elevation. Distance to dam was classified 10 km apart.

Many methods have been used for geological hazard

susceptibility assessments and mapping (Pardeshi et al., 2013). In this study, we selected the information value method (IVM) for the CLs susceptibility assessment. IVM is an indirect bivariate statistical approach that is

fit for assessing the geological hazards susceptibility in an objective manner, and it offers extensive application for geological disaster assessment (Wu et al., 2001; Wu et al., 2004; Chen et al., 2016; Ba et al., 2017; Du et al., 2017). Specifically, the IVM is used to calculate the ratio between the weight of each class of factor layer of CLs density or area for each subclass to the total CLs density or area in a specific region (Du et al., 2017). In general, CLs will possibly occur in those sites which have the same conditions as those where such hazards occurred previously (Lee and Pradhan, 2006). Thus, we used the IVM to estimate the spatial relationship between the conditioning factor with different classes and the probability of CLs occurrence in this study. The higher the information value, the stronger the relationship between the probability of a CLs occurrence and the conditioning factor class (Ba et al., 2017). The information value can be calculated with Equ. 1:

$$I_i = \log \frac{N_i / N}{S_i / S} \quad (1)$$

where N_i is the number of units for CLs of factor class i , N is the total number of units of occurred CLs, S_i is the total area of all CLs, and S is total number of units in the study region.

Generally, there are many influencing factors affecting CLs susceptibility for each evaluation unit and different factors exist in several conditions. Here, in order to obtain the CLs susceptibility index, the information value for all conditioning factors were overlaid using the spatial analysis in ArcGIS 10.3 according to Equ. 2.

$$I = \sum_{i=1}^n I_i = \sum_{i=1}^n \log \frac{N_i / N}{S_i / S} \quad (2)$$

where I is the susceptibility index of CLs that denotes the relative susceptibility level, I_i represents the information value of factor i , and n indicates the number of conditioning factors. The results of this CLs susceptibility assessment were divided into five groups using the process of natural breakpoint in ArcGIS 10.3, namely very low, low, moderate, high and very high landslide susceptibility.

After referencing other scholars' experiences of the evaluation index (Wu et al., 2001, 2004; Du et al., 2017) and considering the availability and accuracy of the dataset, the factors including elevation, slope gradients, aspects, lithology, distance to dam and precipitation in

wet season (May to October) were selected for CLs susceptibility assessment. The classifications of elevation, slope gradient, slope aspect and river longitudinal distances to dam site are the same as those of the aforementioned WLFZ and CLs distribution. Based on a 1:500 000 geological map and field investigation, this study differentiated lithology features into eight stratigraphic systems, namely Jurassic (J1–3), Cretaceous (K), Silurian (S), Triassic (T3), Permian (P2), Devonian (D1), Carboniferous (C1) and Sinian (Ptch). The average precipitation of wet season was collected from eight counties' weather stations along the XWR region. Then, the kriging interpolation method was used to create a precipitation contour map of the XWR area, which was overlaid with the map of WLFZ distribution to ascertain the precipitation distribution. A 10 m × 10 m grid cell was used as the basic unit for the evaluation of CLs susceptibility based on the spatial resolution of DEM.

3 Results

3.1 The distribution of water-level-fluctuating zone

The total area of the WLFZ in the XWR is 87.03 km², with 48.46 km² in the mainstream of the LCR and 38.57 km² of the HHR, respectively. The two largest areas of WLFZ are located in Fengqing and Changning counties, accounting for more than half of the total WLFZ area, followed by the counties of Yongping and Weishan (Table 2). The areas of WLFZ located in the Longyang district of Baoshan, Nanjian, Yangbi and Yunlong counties are relatively small. According to the scale of 10 km-interval distances to the dam site, the area for nearly all sections is greater than 2 km², except for the segments of the backwater terminal of the HHR and the LCR. The maximum WLFZ area is distributed in sections of 30–40 km and 50–60 km distance to the dam site along the LCR and HHR, respectively (Fig. 4a). In terms of elevation, the WLFZ both in the LCR and the HHR is mainly distributed at elevations ranging from 1190–1200 m, 1210–1220 m and 1230–1240 m, where the area is more than 18 km² for each elevation and adds up to over 60% of the total WLFZ area (Fig. 4b). In general, slope degree of riparian zone in the XWR is mainly below 35°, with acreage of gentle slope less than 15° and steep slopes of 25°–35° accounting for more than 60% of the total WLFZ area (Fig. 4c). There is no substantial difference in WLFZ distribution within slope

Table 2 Distribution of the water-level-fluctuating zone (WLFZ) along the the Xiaowan Reservoir in different administrative regions

Counties	Area of WLFZ (km ²)	Proportion (%)
Yunlong	0.29	0.33
Yongping	13.14	15.10
Yangbi	2.91	3.34
Weishan	11.39	13.09
Nanjian	5.11	5.87
Longyang	6.92	7.95
Changning	20.62	23.69
Fengqing	26.65	30.62
Total	87.03	100

gradients ranging from 0–35° between the LCR and the HHR, while WLFZ is mainly distribute in the main-stream of the LCR for high steep slope (35°–45°) and cliff (> 45°). For slope aspects, WLFZ areas at a flat slope, northeast, and southwest slope account for 17.55%, 13.39% and 13.20% of total area, respectively. The same WLFZ distribution trends with bank aspects was observed for both the LCR and the HHR (Fig. 4d).

3.2 The distribution of collapses and landslides along the riparian zone

From 2008 to 2014, as many as 804 individual CLs masses (691 along the LCR and 113 on the HHR) covering a total area of 1.98 km² have been identified in the riparian zone of XWR. The spatial distribution of CLs along stream segments, elevations, slope gradients and aspects are presented in Fig. 5.

Fig. 5a showed area and density of CLs with 10 km apart along the riparian zone appear with no consistent trend. The maximum CLs area is distributed at the segment 0–10 km distant from the dam, while the highest CLs density is located at 150–160 km. Notably, the CLs densities at 130–180 km and 0–10 km sections were significantly higher than those at other reaches of the XWR. Regarding elevation, CLs are mainly distributed in the altitude ranges of 1210–1240 m, with an area accounting for nearly 65% of the total CLs area of the XWR's riparian zone (Fig. 5b). As the elevation changes, the area of CLs gradually increases at the elevations of 1180–1220 m, and then slowly decreases. Meanwhile, the CLs density also increases rapidly along with the increase in elevation, although it drops sharply

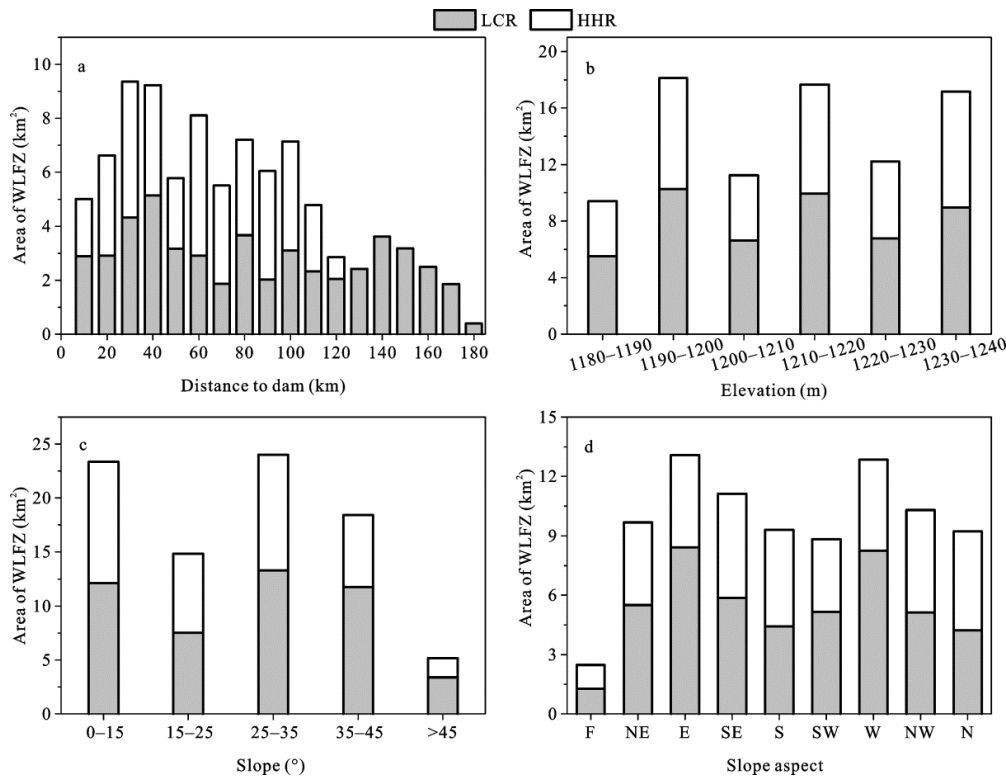


Fig. 4 Distribution of the water-level-fluctuating zone (WLFZ) in the Xiaowan Reservoir area (a. Distance to dam site; b. Elevation; c. Slope gradient; d. Slope aspect; F, flat; N, North; NE, Northeast; E, East; SE, Southeast; S, South; SW, Southwest; W, West; NW, Northwest; LCR, Lanchang River; HHR, Heihui River)

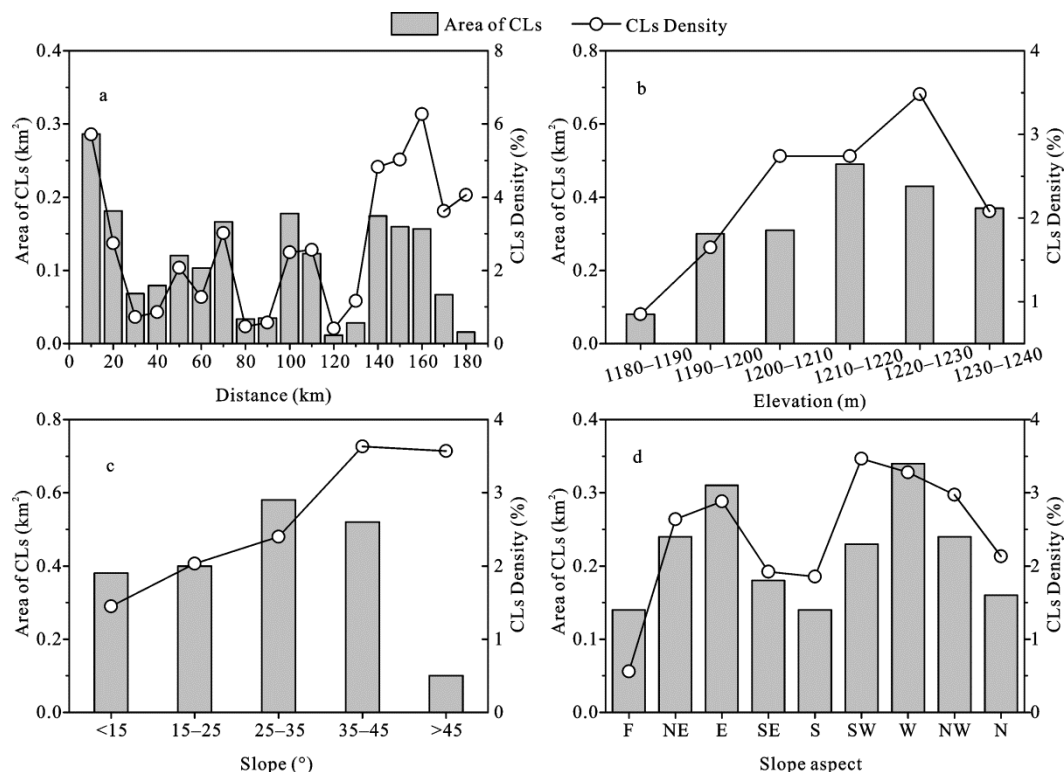


Fig. 5 Collapses and landslides (CLs) number and density distribution along the water-level-fluctuating zone (WLFZ) of Xiaowan Reservoir with different conditioning factors classes. (a. Distance to dam site; b. Elevation; c. Slope gradient; d. Slope aspect; F, flat; N, North; NE, Northeast; E, East; SE, Southeast; S, South; SW, Southwest; W, West; NW, Northwest)

at the elevation of 1230–1240 m. In terms of the slope gradients, the largest CLs area is distributed in the slope degree of 25°–35°, followed by the slope of 35°–45°, and the smallest CLs area is distributed in the slope degree of > 45° (Fig. 5c). However, the CLs density increases obviously with a corresponding increase in the slope degree. In the case of the slope aspect, the CLs generally occur at the aspects of easterly direction (east and northeast) and westerly direction (west, southwest and northwest), probably because these directions are roughly perpendicular to the northwest and southeast direction of the LCR, and thus exposed to stronger reservoir water fluctuations or affected by the orientation of discontinuities controlling bank stability (Fig. 5d). Furthermore, the maximum CLs density appears in the southwesterly direction (3.10%), followed by the westerly direction (2.96%), and the minimum density certainly occurs at the flat slope areas.

3.3 Susceptibility of the collapses and landslides

3.3.1 Information value and susceptibility mapping

In this study, factors of topography, water and geology

were selected to conduct the IVM process. The information values of different evaluation indicators were calculated and then added together using Equ. 2. The statistical results indicate that the total information value for CLs susceptibility of the WLFZ in the XWR is between –2.74 and 1.90. In this study, respective IVM were defined in a range for susceptibility hazard zones $I < -1.13$, very low; $-1.13 < I < -0.50$, low; $-0.50 < I < 0.03$, moderate; $0.03 < I < 0.60$, high and $I > 0.6$, very high. Mapping results demonstrated that the moderate susceptibility zone has the largest area, with 26.64 km², followed by the high and low susceptibility zones, with 20.76 km² and 19.66 km², respectively. The corresponding areas of very high and very low susceptibility zones are 10.66 km² and 9.31 km², respectively. The combined area of high and very high susceptibility zones account for more than 36.10% of the total WLFZ area, while the combine area of very low and low susceptibility zones account for 33.29%. Fig. 6 illustrates that many sections of the WLFZ are located in the very high danger zone. Specifically, the very high susceptibility zones are located mostly in the sections of Wayao

to Shuizhai, Datianba, Mangshui to Dashi townships and the riparian zone close to the dam of the LCR, as well as the sections of dam site to upstream of 10 km (including Qianghua and Xiaowandong towns), Yongxin to Shili, and Jijie towns along the HHR (Fig. 6).

3.3.2 The CLs susceptibility zonation compared with the actual CLs distribution

The CLs susceptibility zonation results with IVM were compared with the actual CLs distribution from remote sensing interpretation. Fig. 7 illustrates that both the area and density of CLs have increased with the rise in susceptibility levels; particular CLs density in the very highly susceptible group has increased dramatically. Statistical results revealed that the area of above-high hazard zones accounts for 58.08% of the total CLs area, while the area of very low and low susceptibility zones only accounts for 17.68%. The WLFZ area of high and very high danger zones cover approximately one third of the total WLFZ area of the XWR, whereas its CLs area accounts for 54.46% of the total CLs area. The actual

CLs area in the very high susceptibility zone is the largest, although the corresponding WLFZ area is small (Fig. 7). Therefore, the mapping zones are basically consistent with the actual CLs distribution according to the remote sensing interpretation and the field investigation, indicating that the IVM is practicable to evaluate the susceptibility of CLs in the riparian zone of the XWR.

4 Discussion

4.1 The spatial distribution of water-level-fluctuating zone and collapses and landslides in the Xiaowan Reservoir

The riparian zone in mega reservoirs have attracted increasing attention since the formation of the WLFZ in the Three Gorges Reservoir (TGR) in China. As the largest hydropower project in the world, after TGR full implementation in 2008, an artificial riparian region with a vertical elevation difference of 30 m and a total area of 349 km² have been created (Fu et al. 2010; Ye et

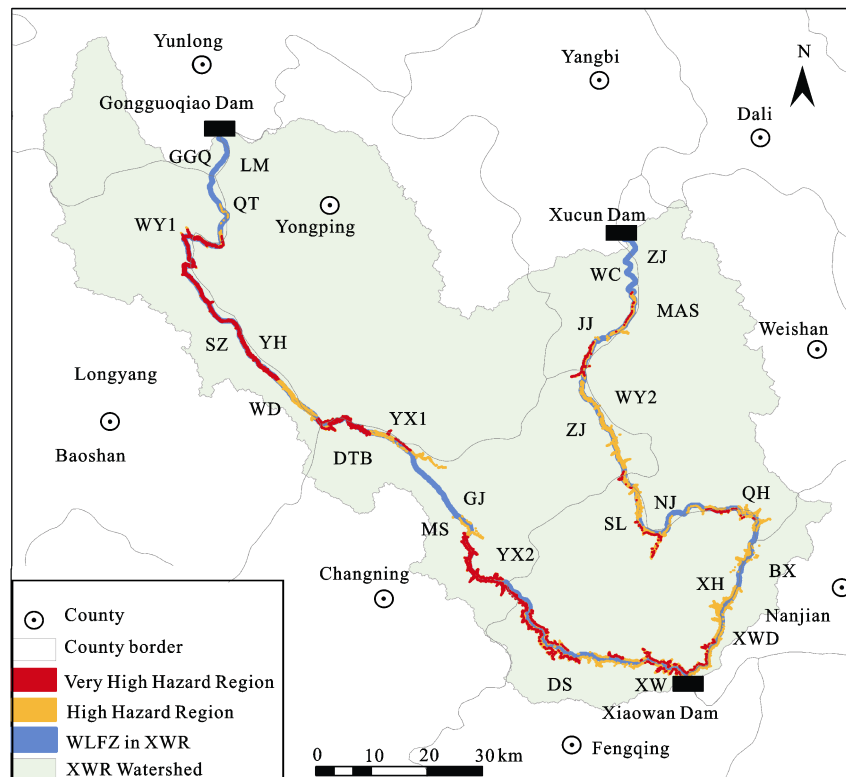


Fig. 6 Distribution of high and very high collapses and landslides hazard regions along the water-level-fluctuating zone of Xiaowan Reservoir (the capital letters represent the towns along the Xiaowan Reservoir, including Xiaowan – XW, Dashi – DS, Yongxin – YX1, Mangshui – MS, Goujie – GJ, Datianba – DTB, Yongxie – YX2, Wadu – WD, Yonghe – YH, Shuizhai – SZ, Wayao – WY1, Qutong – QT, Longmen – LM and Gongguoqiao – GGQ towns in the mainstream of LCR, and Xiaowandong – XWD, Xinhua – XH, Bixi – BX, Qinghua – QH, Niujie – NJ, Shili – SL, Zhuojie – ZJ, Wuyin – WY2, Jijie – JJ, Maanshan – MAS, Wachang – WC and Zijin – ZJ towns in the HHR).

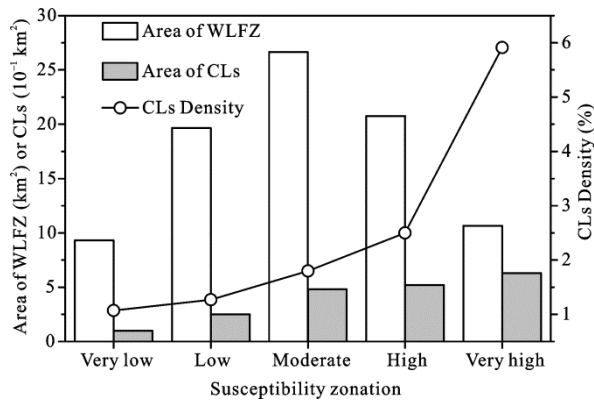


Fig. 7 The area of collapses and landslides and the water-level-fluctuating zone distribution in the different collapses and landslides susceptibility zones in the Xiaowan Reservoir

al. 2011; Tang et al. 2014). At present, research on the environment impact of the WLFZ is still concentrated primarily in the TGR, due to its large area of WLFZ and severe ecological and environmental degradation (Zhou et al., 2010; Li et al., 2013; Wang et al., 2014; Tang et al., 2016; Su et al., 2017). Compared with the TGR, the XWR area, reservoir capacity and the backwater length are on a much smaller scale, even though the water level variation range of 60 m in the XWR is twice that of the TGR (Table 3). Obviously, the difference in area of WLFZ is closely related to the bank topography. The submerged zone of the TGR has a mass of sloping fields, paddy fields, homesteads and other gentle slopes, and thus over 62.00% area of the WLFZ is less than 15°, while the area ratio of steep slope is only 14.58% (Yuan et al., 2013). In contrast, the WLFZ with a gentle slope in the XWR account for less than a third of its total area, whereas the proportion of steep slope area is more than 50% (Table 3). In addition, the bank in the TGR is dominated by a soil type with a mixture of soil and rock in the west of Fengjie County, while the bank structure in the east of Fengjie is mainly rock (Bao et al., 2015). Compared to the TGR, the riparian zone of the XWR is composite of a mixture of soil, rock and rock-soil, with

a large amount of loose deposits (Li, 2011).

The diverse landforms also cause different types of geological disaster in the riparian zone. The primary geohazards type in the WLFZ of the TGR is landslide, followed by bank collapse, while dangerous rock and debris flows also occur in some segments (Zhou, 2008). However, geohazards in the XWR are dominated by bank collapse and landslide due to the complexity of the geological environment; debris flow disasters have not yet been reported. The XWR area is located in the alpine and canyon region with steep mountain slopes, numerous original unstable reservoir sections are resulting from the developed karst landform and active new tectonic movement. The present study found that more than 800 CLs masses have been observed since the complete impoundment of the XWR. Both the number and area of CLs change in relation to their distance to the dam site, which is closely related to the range of water level fluctuation at different bank sections. Generally, the closer the dam site, the larger WLFs of the reservoir (Fig. 8). Based on the DEM of the XWR, the lowest elevations of the LCR and the HHR were extracted and then converted to approximate the maximum water level lines. The results revealed that the maximum WLFs was maintained for up to 127 km in the LCR and 87 km in the HHR from the dam site respectively, after which the water levels began to decline until the end of the backwater was close to 0 (Fig. 8). It is clear that with a decrease in WLFs, the reconstructive role of the reservoir water on bank gradually weaken, so that the number of CLs away from the dam site will be relatively small. The significant difference between number of CLs occurrence in LCR and HHR can be explained by the different geomorphology, WLFs, vegetation cover, climate and intensity of human activity. However, more detailed investigations are needed to reveal this difference. Actually, the zone with a high CLs area is not always consistent with a large number of CLs (Fig. 9), which may result from the different sizes of the CLs masses.

Table 3 Main features of the Xiaowan Reservoir and the Three Gorges Reservoir

	Basin	SC (×10 ⁹ m ³)	TA (km ²)	BL (km)	WLFs (m.s.l.)	AWLFZ (km ²)	WDPS (%)		
							< 15°	15°–25°	>25°
TGR	Yangtze River	39.30	1084.00	663.00	145–175	349.00	62.28	23.14	14.58
XWR	Lancang River	15.00	193.98	179.60	1180–1240	87.03	27.21	17.32	55.47

Notes: the capital letters of SC, TA, BL, WLFs, AWLFZ and WDPS represent the storage capacity, total area, backwater length, water level fluctuations, the area of the water-level-fluctuating zone (WLFZ), and WLFZ distribution proportion in different slope degrees, respectively; m.s.l is mean sea level. Data of the Three Gorges Reservoir were from Yuan et al. (2013) and Tang et al. (2015).

Meanwhile, with an increase in elevation, the area of CLs decreased at first and then increased (Fig. 5b). At the elevation of 1180–1190 m, the CLs area is very small; this result may be associated with the occurrence of sedimentation in the low altitude region. Large amount of sediment deposition from upstream, as well as soil and rock from topsoil erosion and CLs at the upper part of the WLFZ may prevent the occurrence of large-scale collapses, landslides and soil erosion in the low elevation regions of the riparian zone (Su et al., 2017). However, after the elevation up to 1190 m, the CLs area increased markedly due to the decrease of water flooding intensity. At the same time, the CLs density increased dramatically with the increase in altitude of 1190 m to 1240 m (Fig. 5b), which illustrating that the riparian zone along this height range is prone to collapse. The area of CLs and WLFZ in different slope gradients and aspects has a significantly positive correlation at the significant level of 0.01 (Fig. 5c and 5d). As the slope degrees rise, the CLs density increases significantly, which indicates that the slope factor is an important topographic factor in determining the occurrence of CLs (Fig. 5c). With regard to slope aspects, CLs distributed in all directions, including the biggest CLs area occur in easterly and westerly directions which approximately perpendicular to the course of the river and thus contribute to bank failure (Dai and Lee, 2002; Lee and Sambath, 2006). The southwest slope is also prone to geological hazards with the highest CLs density. The IVM results revealed that numerous segments of the riparian zone in the XWR are located in the high and very high CLs susceptibility regions, with a developed CLs frequency and density (Fig. 6).

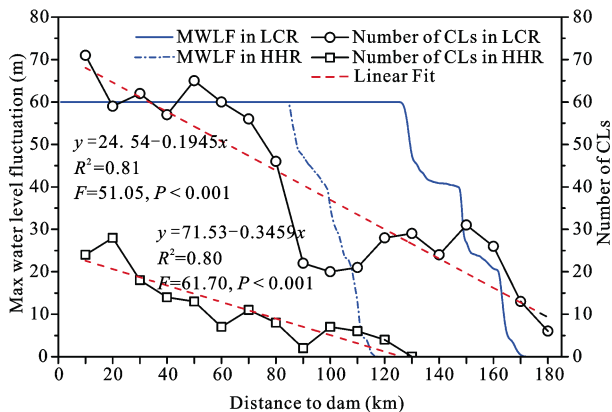


Fig. 8 Max water level fluctuation (MWLF) and number of collapses and landslides distribution along the Xiaowan Reservoir (LCR, Lanchang River; HHR, Heihui River)

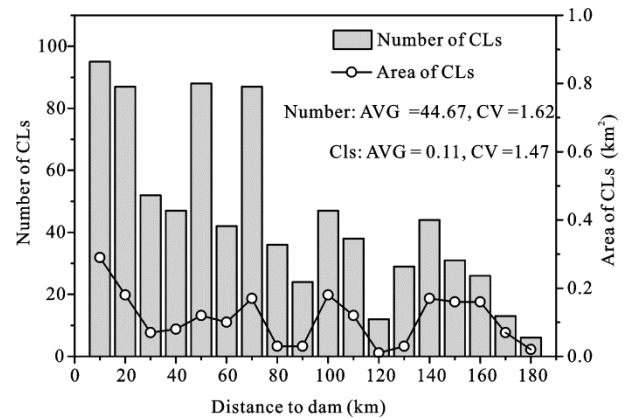


Fig. 9 The area and number of collapses and landslides (CLs) changes along with distance to the the Xiaowan dam

4.2 The influence of water level fluctuations (WLFs) on the bank stability

Bank stability is closely associated with the hydraulic conductivity of rock-soil masses and the range of reservoir WLFs (Xia et al., 2015). As the water level fluctuates, the hydraulic conductivity of rock-soil and the groundwater level are notably altered; these two factors directly influence bank stability (Fujita, 1977; Yan et al., 2010). During reservoir impounding, if the hydraulic conductivity of soil and rock masses is very high, the groundwater table along the bank increases in step with the reservoir water level, thus resulting in an increase in pore water pressure in the soil and rock masses and thereby reduce the bank stability (Fujita, 1977; Xia et al., 2015; Jiang et al., 2016). Conversely, when the hydraulic conductivity is relatively low, the rising reservoir water level will pull ahead of the groundwater level, thus increasing seepage pressure on the soil and rock masses, which is beneficial to the slope's stability (Yan et al., 2010; Xia et al., 2015). Accordingly, during the process of reservoir discharge, the groundwater table will keep in step with the lowering reservoir water level when it is equal to or drops below the hydraulic conductivity, thus increasing the bank stability (Zhang et al., 2006; Xia et al., 2015). In contrast, when the descending rate of water level is higher than the hydraulic conductivity of soil and rock, the decreasing groundwater table will fall behind that of the reservoir water level; This process will produce a strong hydrodynamic pressure directly into the soil-rock masses and ultimately reduce the bank stability (Fujita, 1977; Xia et al., 2015; Sun et al., 2017b). Additionally, the falling water level produces a significant penetration in the rock-soil body,

further contributing to the sharp decrease in sliding resistance and the significant increase in sliding force, all of which create the potential for geological disasters such as collapses and landslides (Liao et al., 2005; Wang and Yan, 2007; Zhou et al., 2010). This is why, after the impoundment of the XWR, the dramatic fluctuations in the water level have greatly affected its bank stability. As a result, a large number of CLs masses have occurred in the WLFZ of the XWR (Figs. 8 and 9). A significant correlation between WLFs and the number of CLs can be demonstrated in Fig. 8, although it may not follow the same trend, which implying the significant influence of WLFs on the bank stability.

4.3 The application of collapses and landslides susceptibility zonation in the Xiaowan Reservoir

Since the beginning of the impoundment of the XWR in December 2008, many serious geological hazards have been noted on both sides of the reservoir bank. These disasters have not only seriously affected the operation and safety of the reservoir and dam but have also caused great damage and threats to the production and life of the inhabitants of the reservoir region. The Huangtian landslide that occurred on 20 July 2009 at the right bank of LCR about 7.5 km upstream of XWD resulted in the death of two people and a left of 12 missing people. A large quantity of slumped mass reduces the storage capacity of the XWR, also negatively influencing the normal power generation and flood control capabilities of the XWD. Therefore, the evaluation of CLs susceptibility in the XWR area, especially in the riparian zone, is critical to the prevention and control of regional geological disasters. Thorough CLs assessment and zonation can be used to carry out targeted monitoring and control work of the geohazards of the XWR. For this reason, relevant departments have carried out investigations and monitoring of the bank deformation and instability, before and after the XWR impoundment. Particularly, following the complete filling of the XWR, the power station management department conducted a long-term inspection of the bank collapse, landslide and other geological hazard points, using artificial observations combined with GPS automatic real-time monitoring (Chen et al., 2015b). In this study, we investigated the number and area of CLs occurring on the WLFZ of the XWR, based on remote sensing image interpretation together with a field survey, and further conducted an

assessment and mapping of susceptibility using the IVM. The results sufficiently reflect the CLs that have occurred in the riparian zone of XWR. Therefore, the results of this study may confidently be used as a reference for relevant departments, especially the reservoir management division, to carry out targeted monitoring and control of the potential geohazards at the XWR. For high susceptibility groups, especially in the very high susceptibility zone, monitoring density and frequency should be strengthened, and appropriate measures taken to prevent and control bank failure. At the same time, disaster prevention training, information and awareness levels should be enhanced amongst the residents of townships and cities in the XWR. The moderate susceptibility zone should also be monitored and prevented, along with a steady watch over even the low and extremely low hazard areas.

The method of CLs survey and susceptibility mapping used in this paper provided a convenient, quick and safe way to investigate and explore the geological hazards of the reservoir in the alpine valley region. This model can therefore be applied to geological hazard investigation and study of the reservoir in other areas. It is important to note that the geological hazards investigation and evaluation results in the WLFZ used this model still requires further validation in practical application, in order to ensure the veracity and reliability of evaluation results. In particular, the typical bank collapse and landslide disasters need to be verified via field investigations and evaluations.

5 Conclusions

The full impoundment of the XWR created an artificial riparian zone with a vertical height of 60 m and the total area of 87.03 km² of the WLFZ (48.46 km² in the mainstream of the LCR and 38.57 km² in the HHR, respectively). As many as 804 CLs masses, with a total area of 1.98 km², have been identified based on the remote-sensing images of GF-1 and Google Earth. The CLs mainly occurred in the regions with the elevation of 1190–1240 m and the slope gradient of 25°–45°. Also, the CLs density ratio increases significantly with the increase in elevation and slope degree. The results of CLs susceptibility assessment used the information value method to indicate that many segments of the XWR are in the high or very high susceptibility zones,

whereas mainly distributed in the lithology of Silurian formation, and mostly characterized by higher elevations, steeper slopes, slopes vertical to the strike of the LCR and within close distance to the dam site. The results of susceptibility mapping in this study are consistent with the actual CLs distribution in the riparian zone of the XWR. This study also demonstrated that the WLFs play a critical role in bank instability, although more detailed research is needed. Generally, the consequences in this paper can be applied to the prevention and controlling of CLs hazards in the riparian zone of XWR. Furthermore, the method used for the reservoir riparian zone geological hazard investigation and assessment in this study has been found to be convenient, quick and safe to use in the investigation and exploration of the potential geological hazards of the reservoir in the southwest alpine gorge area of China.

References

- Alimohammadlou Y, Najafi A, Yalcin A, 2013. Landslide process and impacts: a proposed classification method. *Catena*, 104: 219–232. doi: 10.1016/j.catena.2012.11.013
- Ba Q Q, Chen Y M, Deng S S et al., 2017. An improved information value model based on gray clustering for landslide susceptibility mapping. *ISPRS International Journal of Geo-Information*, 6(1): 1–20. doi: 10.3390/ijgi6010018
- Babanouri N, Dehghani H, 2017. Investigating a potential reservoir landslide and suggesting its treatment using limit-equilibrium and numerical methods. *Journal of Mountain Science*, 14(3): 432–441. doi: 10.1007/s11629-016-3898-2
- Bao Y H, Gao P, He X B, 2015. The water-level fluctuation zone of Three Gorges Reservoir—A unique geomorphological unit. *Earth-Science Reviews*, 150: 14–24. doi: 10.1016/j.earscirev.2015.07.005
- Bao Yuhai, He Xiubin, 2011. Preliminary study on soil erosion at the water-level -fluctuating zone of the Three-Gorges Reservoir. *Research of Soil and Water Conservation*, 18(6): 190–195. (in Chinese)
- Barla G, Paronuzzi P, 2013. The 1963 Vajont landslide: 50th anniversary. *Rock Mechanics and Rock Engineering*, 46(6): 1267–1270. doi: 10.1007/s00603-013-0483-7
- Butt M J, Mahmood R, Waqas A, 2011. Sediments deposition due to soil erosion in the watershed region of Mangla Dam. *Environmental Monitoring and Assessment*, 181(1–4): 419–429. doi: 10.1007/s10661-010-1838-0
- Chai Zongxin, 1996. Bank erosion and control. *Journal of Catastrophology*, 11(3): 27–31. (in Chinese)
- Chang X L, Liu X H, Zhou W, 2010. Hydropower in China at present and its further development. *Energy*, 35(11): 4400–4406. doi: 10.1016/j.energy.2009.06.051
- Chen T, Niu R Q, Du B et al., 2015a. Landslide spatial susceptibility mapping by using GIS and remote sensing techniques: a case study in Zigui County, the Three Georges reservoir, China. *Environmental Earth Sciences*, 73(9): 5571–5583. doi: 10.1007/s12665-014-3811-7
- Chen Weidong, Yin Yunkun, Zhu Tingxing, 2015b. Discussion on reservoir bank management of Xiaowan hydropower station. *Water Power*, 41(10): 12–14. (in Chinese)
- Chen Z, Han F, Chen Z et al., 2015c. *Final Acceptance Report of the Environmental Protection after the Completion of Xiaowan Hydropower station on Lancang River*. Environmental Engineering Assessment Center of Ministry of environmental protection of the People's Republic of China. (in Chinese)
- Chen T, Niu R Q, Jia X P, 2016. A comparison of information value and logistic regression models in landslide susceptibility mapping by using GIS. *Environmental Earth Sciences*, 75: 867. doi: 10.1007/s12665-016-5317-y
- Cyberski J, 1973. Erosion of banks of storage reservoirs in Poland. *Hydrological Sciences Bulletin*, 18(3): 317–320. doi: 10.1080/02626667309494042
- Dai F C, Lee C F, 2002. Landslide characteristics and slope instability modeling using GIS, Lantau Island, Hong Kong. *Geomorphology*, 42(3–4): 213–228. doi: 10.1016/S0169-555X(01)00087-3
- Du G L, Zhang Y S, Iqbal J et al., 2017. Landslide susceptibility mapping using an integrated model of information value method and logistic regression in the Bailongjiang watershed, Gansu Province, China. *Journal of Mountain Science*, 14(2): 249–268. doi: 10.1007/s11629-016-4126-9
- Duan X W, Gu Z J, Li Y G et al., 2016. The spatiotemporal patterns of rainfall erosivity in Yunnan Province, southwest China: An analysis of empirical orthogonal functions. *Global and Planetary Change*, 144: 82–93. doi: 10.1016/j.gloplacha.2016.07.011
- Fu B J, Wu B F, Lu Y H et al., 2010. Three gorges project: efforts and challenges for the environment. *Progress in Physical Geography*, 34(6): 741–754. doi: 10.1177/0309133310370286
- Fujita H, 1977. Influence of water level fluctuations in a reservoir on slope stability. *Bulletin of the International Association of Engineering Geology-Bulletin de l'Association Internationale de Géologie de l'Ingénieur*, 16(1): 170–173. doi: 10.1007/BF02591474
- Guo C, Montgomery D R, Zhang Y et al., 2015. Quantitative assessment of landslide susceptibility along the Xianshuihe fault zone, Tibetan Plateau, China. *Geomorphology*, 248: 93–110. doi: 10.1016/j.geomorph.2015.07.012
- Huang B L, Yin Y P, Liu G N et al., 2012. Analysis of waves generated by Gongjiafang landslide in Wu Gorge, three Gorges reservoir, on November 23, 2008. *Landslides*, 9(3): 395–405. doi: 10.1007/s10346-012-0331-y
- Iverson R M, 2000. Landslide triggering by rain infiltration. *Water Resources Research*, 36(7): 1897–1910. doi: 10.1029/2000WR900090
- Jia G W, Zhan T L T, Chen Y M et al., 2009. Performance of a large-scale slope model subjected to rising and lowering water levels. *Engineering Geology*, 106(1–2): 92–103. doi: 10.1016/

- j.enggeo.2009.03.003
- Jiang Q H, Wei W, Xie N et al., 2016. Stability analysis and treatment of a reservoir landslide under impounding conditions: a case study. *Environmental Earth Sciences*, 75: 2. doi: 10.1007/S12665-015-4790-Z
- Johansson J, Edeskär T, 2014. Effects of external water-level fluctuations on slope stability. *The Electronic Journal of Geotechnical Engineering*, 19: 2437–2463.
- Kaczmarek H, Mazaeva O A, Kozyreva E A et al., 2016. Impact of large water level fluctuations on geomorphological processes and their interactions in the shore zone of a dam reservoir. *Journal of Great Lakes Research*, 42(5): 926–941. doi: 10.1016/j.jglr.2016.07.024
- Lee S, Pradhan B, 2006. Probabilistic landslide hazards and risk mapping on Penang Island, Malaysia. *Journal of Earth System Science*, 115(6): 661–672. doi: 10.1007/s12040-006-0004-0
- Lee S, Sambath T, 2006. Landslide susceptibility mapping in the Damrei Romel area, Cambodia using frequency ratio and logistic regression models. *Environmental Geology*, 50(6): 847–855. doi: 10.1007/s00254-006-0256-7
- Li H, 2012. *Bank Slope Risk Assessment on The Reservoir Region of Xiaowan Reservoir Based on RS and GIS*. Chengdu: Chengdu University of Technology, Chendgu. (in Chinese)
- Li Pengyue, 2011. *Study on Bank Collapse's Type and Mechanism in Mountain Reservoir—A Case of Xianwan Reservoir*. Chendgu: Chengdu University of Technology. (in Chinese)
- Li K F, Zhu C, Wu L et al., 2013. Problems caused by the three gorges dam construction in the Yangtze River basin: a review. *Environmental Reviews*, 21(3): 127–135. doi: 10.1139/Er-2012-0051
- Liao Hongjian, Sheng Qian, Gao Shihang et al., 2005. Influence of drawdown of reservoir water level on landslide stability. *Chinese Journal of Rock Mechanics and Engineering*, 24(19): 3454–3458. (in Chinese)
- Liu Y., Huang R, and Deng H, 2011. Stability of Xinminbazi Landslide Located in Xiaowan Hydropower Station Reservoir Region. *Journal of Mountain Science*, 29(3): 328–336.
- Luo Hongming, Tang Huiming, Zhang Guangcheng et al., 2008. The influence of water level fluctuation on the bank landslide stability. *Earth Science—Journal of China University of Geosciences*, 33(5): 687–692. (in Chinese)
- Pardeshi S D, Autade S E, Pardeshi S S, 2013. Landslide hazard assessment: recent trends and techniques. *SpringerPlus*, 2: 523. doi: 10.1186/2193-1801-2-523
- Park N W, 2010. Application of Dempster-Shafer theory of evidence to GIS-based landslide susceptibility analysis. *Environmental Earth Sciences*. 62(2): 367–376. doi: 10.1007/s12665-010-0531-5
- Paronuzzi P, Bolla A, 2012. The prehistoric Vajont rockslide: an updated geological model. *Geomorphology*, 169–170: 165–191. doi: 10.1016/j.geomorph.2012.04.021
- Paronuzzi P, Rigo E, Bolla A, 2013. Influence of filling- drawdown cycles of the Vajont reservoir on Mt. Toc slope stability. *Geomorphology*, 191: 75–93. doi: 10.1016/j.geomorph.2013.03.004
- Pradhan B, Lee S, 2010. Landslide susceptibility assessment and factor effect analysis: backpropagation artificial neural networks and their comparison with frequency ratio and bivariate logistic regression modelling. *Environmental Modelling & Software*, 25(6): 747–759. doi: 10.1016/j.envsoft.2009.10.016
- Saint-Laurent D, Touileb B N, Saucet J P et al., 2001. Effects of simulated water level management on shore erosion rates. Case study: Baskatong Reservoir, Québec, Canada. *Canadian Journal of Civil Engineering*, 28(3): 482–495. doi: 10.1139/101-018
- Song K, Yan E C, Zhang G D et al., 2015. Effect of hydraulic properties of soil and fluctuation velocity of reservoir water on landslide stability. *Environmental Earth Sciences*, 74(6): 5319–5329. doi: 10.1007/s12665-015-4541-1
- Su X L, Nilsson C, Pilotto F et al., 2017. Soil erosion and deposition in the new shorelines of the three gorges reservoir. *Science of the Total Environment*, 599–600: 1485–1492. doi: 10.1016/j.scitotenv.2017.05.001
- Sun G H, Yang Y T, Cheng S G et al., 2017a. Phreatic line calculation and stability analysis of slopes under the combined effect of reservoir water level fluctuations and rainfall. *Canadian Geotechnical Journal*, 54(5): 631–645. doi: 10.1139/cgj-2016-0315
- Sun G H, Yang Y T, Jiang W et al., 2017b. Effects of an increase in reservoir drawdown rate on bank slope stability: A case study at the Three Gorges Reservoir, China. *Engineering Geology*, 221: 61–69. doi: 10.1016/j.enggeo.2017.02.018
- Tang Q, Bao Y H, He X B et al., 2016. Flow regulation manipulates contemporary seasonal sedimentary dynamics in the reservoir fluctuation zone of the Three Gorges Reservoir, China. *Science of the Total Environment*, 548–549: 410–420. doi: 10.1016/j.scitotenv.2015.12.158
- Tang Q, Bao Y H, He X B et al., 2014. Sedimentation and associated trace metal enrichment in the riparian zone of the Three Gorges Reservoir, China. *Science of the Total Environment*, 479–480: 258–266. doi: 10.1016/j.scitotenv.2014.01.122
- Tang Q, Fu B J, Collins A L et al., 2017. Developing a sustainable strategy to conserve reservoir marginal landscapes. *National Science Review*, 5(1): 10–14. doi: 10.1093/nsr/nwx102
- Tang W Z, Li Z Y, Qiang M S et al., 2013. Risk management of hydropower development in China. *Energy*, 60: 316–324. doi: 10.1016/j.energy.2013.08.034
- Wang H B, Xu W Y, Xu R C et al., 2007. Hazard assessment by 3D stability analysis of landslides due to reservoir impounding. *Landslides*, 4(4): 381–388. doi: 10.1007/s10346-007-0095-y
- Wang Minghua, Yan Echuan, 2007. Study on influence of reservoir water impounding on reservoir landslide. *Rock and Soil Mechanics*, 28(12): 2722–2725. (in Chinese)
- Wang J, Xiang W, Lu N, 2014. Landsliding triggered by reservoir operation: a general conceptual model with a case study at Three Gorges Reservoir. *Acta Geotechnica*, 9(5): 771–788. doi: 10.1007/s11440-014-0315-2
- Wang T, 2012. *Analysis on revival formation mechanism and hazard of Ximi Landslide in Heihui River Reservoir area of Xiaowan Hydropower Station*. Chengdu: Chengdu University of Technology, Chendgu. (in Chinese)

- Wu Jiahao, 2011. *The Research and Forecasting on the Mountain River-type Slope Surge Hazard—A case of Xiaowan Reservoir*. Chengdu: Chengdu University of Technology, Chengdu. (in Chinese)
- Wu L, Wang Z, 2013. Three Gorges Reservoir water level fluctuation influences on the stability of the slope's analysis. *Advanced Materials Research*, 739, 283–286. doi: 10.4028/www.scientific.net/AMR.739.283
- Wu S R, Shi L, Wang R J et al., 2001. Zonation of the landslide hazards in the foreresservoir region of the Three Gorges Project on the Yangtze River. *Engineering Geology*, 59(1–2): 51–58. doi: 10.1016/S0013-7952(00)00061-2
- Wu S R, Jin Y M, Zhang Y S et al., 2004. Investigations and assessment of the landslide hazards of Fengdu County in the reservoir region of the Three Gorges project on the Yangtze River. *Environmental Geology*, 45(4): 560–566. doi: 10.1007/s00254-003-0911-1
- Wu X D, He D M, Yang G J et al., 2014. Seasonal variability of water quality and metazooplankton community structure in Xiaowan Reservoir of the upper Mekong River. *Journal of Limnology*, 73(1): 167–176. doi: 10.4081/jlimnol.2014.801
- Xia M, Ren G M, Ma X L, 2013. Deformation and mechanism of landslide influenced by the effects of reservoir water and rainfall, Three Gorges, China. *Natural Hazards*, 68(2): 467–482. doi: 10.1007/s11069-013-0634-x
- Xia M, Ren G M, Zhu S S, et al., 2015. Relationship between landslide stability and reservoir water level variation. *Bulletin of Engineering Geology and the Environment*, 74(3): 909–917. doi: 10.1007/s10064-014-0654-0
- Xu C, Dai F C, Xu X W, et al., 2012. GIS-based support vector machine modeling of earthquake-triggered landslide susceptibility in the Jianjiang River watershed, China. *Geomorphology*, 145–146: 70–80. doi: 10.1016/j.geomorph.2011.12.040
- Xu X B, Tan Y, Yang G S, 2013. Environmental impact assessments of the Three Gorges Project in China: Issues and interventions. *Earth-Science Reviews*, 124: 115–125. doi: 10.1016/j.earscirev.2013.05.007
- Yan Z L, Wang J J, Chai H J, 2010. Influence of water level fluctuation on phreatic line in silty soil model slope. *Engineering Geology*, 113(1–4): 90–98. doi: 10.1016/j.enggeo.2010.02.004
- Yang Q, Ye Z, Ding W et al., 2014. Impact of water level fluctuation on the reservoir landslide stability. In: Sassa K, Canuti P, Yin Y (eds). *Landslide Science for a Safer Geoenvironment*. Cham: Springer, 659–664.
- Yalcin A, Reis S, Aydinoglu A C, et al., 2011. A GIS-based comparative study of frequency ratio, analytical hierarchy process, bivariate statistics and logistics regression methods for landslide susceptibility mapping in Trabzon, NE Turkey. *Catena*, 85(3): 274–287. doi: 10.1016/j.catena.2011.01.014
- Ye C, Li S, Zhang Y, et al., 2011. Assessing soil heavy metal pollution in the water-level-fluctuation zone of the Three Gorges Reservoir, China. *J. Hazard Mater*, 191(1): 366–372. doi: 10.1016/j.jhazmat.2011.04.090
- Yilmaz I, 2010. Comparison of landslide susceptibility mapping methodologies for Koyulhisar, Turkey: conditional probability, logistic regression, artificial neural networks, and support vector machine. *Environmental Earth Sciences*, 61(4): 821–836. doi: 10.1007/s12665-009-0394-9
- Yuan X Z, Zhang Y W, Liu H, et al., 2013. The littoral zone in the Three Gorges Reservoir, China: challenges and opportunities. *Environmental Science and Pollution Research*, 20(10): 7092–7102. doi: 10.1007/s11356-012-1404-0
- Zhang Wenjie, Zhan Liangtong, Ling Daosheng, et al., 2006. Influence of reservoir water level fluctuations on stability of unsaturated soil banks. *Journal of Zhejiang University (Engineering Science)*, 40(8): 1365–1370, 1428. (in Chinese)
- Zhong R H, He X B, Bao Y H et al., 2016. Estimation of soil reinforcement by the roots of four post-dam prevailing grass species in the riparian zone of Three Gorges Reservoir, China. *Journal of Mountain Science*, 13(3): 508–521. doi: 10.1007/s11629-014-3397-2
- Zhou Dan, 2008. *The Stabilization Mechanism and Tracking Countermeasures of Water-Level-Fluctuating Zone*. Chongqing: Chongqing Jiaotong University. (in Chinese)
- Zhou Yongjuan, Qiu Jiangxiao, Wang Jiao et al., 2010. A vulnerability assessment of landslide in water-level-fluctuation zones of the Three Gorges Reservoir. *Resources Science*, 30(7): 1301–1307. (in Chinese)
- Zhou J W, Lu P Y, Yang Y C, 2017. Reservoir landslides and its hazard effects for the hydropower station: a case study. In: Mikoš, M, Tiwari B, Yin Y P, et al (eds). *Advancing Culture of Living with Landslides: Volume 2 Advances in Landslide Science*. Cham: Springer, 699–706. doi: 10.1007/978-3-319-53498-581